EJP 108606, revised April 2024

Kinetically anisotropic Hamiltonians: plane waves, Madelung streamlines and superpositions

M V Berry

H H Wills Physics Laboratory, Tyndall Avenue, Bristol BS8 1TL, UK

asymptotico@bristol.ac.uk

Abstract

A Hamiltonian in two space dimensions whose kinetic-energy contributions have opposite signs is studied in detail. Solutions of the time-independent Schrödinger equation for fixed energy are superpositions of plane waves, with wavevectors on hyperbolas rather than circles. The local velocity (e.g. in the Madelung representation) is proportional to the kinetic momentum, i.e. local particle velocity, not the more familiar canonical momentum (phase gradient). The patterns of the associated streamlines are different, especially near phase singularities and phase saddles where the kinetic and canonical streamline patterns have opposite indices. Contrasting with the superficially analogous circular smooth solutions of kinetically isotropic Hamiltonians are wave modes that are anisotropic in position and also discontinuous. Pictures illustrating these phenomena are included. The occurrence of familiar concepts in unfamiliar guises could be useful for teaching quantum or wave physics at graduate level.

Keywords: phase, singularities, index, kinetic, canonical

Submitted to: *Eur.J.Phys*, February 2024, revised April 2024

1. Introduction

When learning and applying elementary quantum mechanics, it is common to consider stationary states of free particles. In two dimensions, waves are (usually complex) functions of position and are influenced by the momentum operator in position representation:

$$\psi = \psi(\boldsymbol{r}), \qquad \boldsymbol{r} = (x, y), \qquad \boldsymbol{p} = -i\nabla_{\boldsymbol{r}}\,, \tag{1.1}$$

The familiar free-particle Hamiltonian is isotropic in the two contributions to the kinetic energy, and the time-independent Schrödinger equation is

$$H_{\text{isotropic}}\psi = \frac{1}{2}\left(p_x^2 + p_y^2\right)\psi = \frac{1}{2}\left(-\partial_{xx}\psi - \partial_{yy}\psi\right) = E\psi. \tag{1.2}$$

This could be written in dimensionless form by expressing distances x, y in units of $E^{-1/2}$, but it is convenient to retain the eigenvalue E. For a quantum particle with mass m, we have used units such that $\hbar^2/m = 1$, equivalent to measuring distances in units of $\hbar/\sqrt{m \times \text{energy}}$.

The aim here is to study what might seem a minor variant, in which the kinetic energies have opposite signs, namely

$$H\psi = \frac{1}{2}\left(p_x^2 - p_y^2\right)\psi = \frac{1}{2}\left(-\partial_{xx}\psi + \partial_{yy}\psi\right) = E\psi. \tag{1.3}$$

But H is very different; we will see that concepts familiar from $H_{\text{isotropic}}$ reappear in H strangely mutated in unexpected forms.

This study originated in the discovery that kinetically anisotropic Hamiltonians describe a special class of 'curl forces', that is, position-dependent Newtonian forces (accelerations) that are not the gradient of a potential [1]. The work reported here describes how kinetically anisotropic Hamiltonians possess distinctive features even in the absence of forces, i.e. for free particles. Moreover, Hamilltonians like H occur in several physical

contexts. In condensed matter, they describe the physics of electrons where the effective mass can have different signs in different directions [2]. In optics, they describe hyperbolic metamaterials [3], in which the dielectric constants can have different signs. And, as will be discussed in section 6, the Schrödinger equation (1.3) can be reinterpreted as the Klein-Gordon equation for a free particle.

In section 2, plane wave solutions of (1.3) are identified, and their unusual dispersion relation emphasised. Section 3 describes the convenient geometrical representation of waves $\psi(\boldsymbol{r})$ in terms of streamlines of momentum (proportional to the local particle velocity) in the Madelung formulation of quantum mechanics [4, 5], currently enjoying a revival [6-8]. The distinction between canonical and kinetic momenta, unimportant for $H_{\text{isotropic}}$ but central to the anisotropic H, is emphasised. Appendix A is a reprise of the Madelung formalism for anisotropic Hamiltonians, with stress on how this naturally involves the kinetic rather than the canonical momentum.

Section 4 describes and illustrates the contrasting geometries of canonical and kinetic streamlines close to phase singularities (nodal points of ψ) and saddle-points of phase $\arg\psi$, explaining how these are fundamentally different for H and $H_{\text{isotropic}}$. Appendix B explores phase extrema; these cannot occur with $H_{\text{isotropic}}$ but can for H, albeit rarely. Section 5 illustrates the rich streamline behaviour that can occur in superpositions of just a few plane waves.

Section 6 derives a solution of the Schrödinger equation (1.3) that is a discontinuous analogue of the smooth solution of its isotropic counterpart (1.2). This phenomenon is demystified by reinterpreting (1.3) as the Klein-Gordon equation.

The concluding section 7 includes a list of concepts whose teaching could be usefully illustrated by the present study.

2. Plane waves

The simplest solutions of (1.3) are momentum eigenstates, i. e. plane waves:

$$\psi_{\boldsymbol{k}}(\boldsymbol{r}) = \exp(i\boldsymbol{k}\cdot\boldsymbol{r}), \qquad \boldsymbol{k} = (k_x, k_y). \tag{2.1}$$

These resemble the familiar plane wave solutions of (1.2), but their dispersion relation is fundamentally different:

$$k_x^2 - k_y^2 = 2E. \tag{2.2}$$

The constant-energy contours in $\boldsymbol{k}$ space are hyperbolas, illustrated in Figure 1.

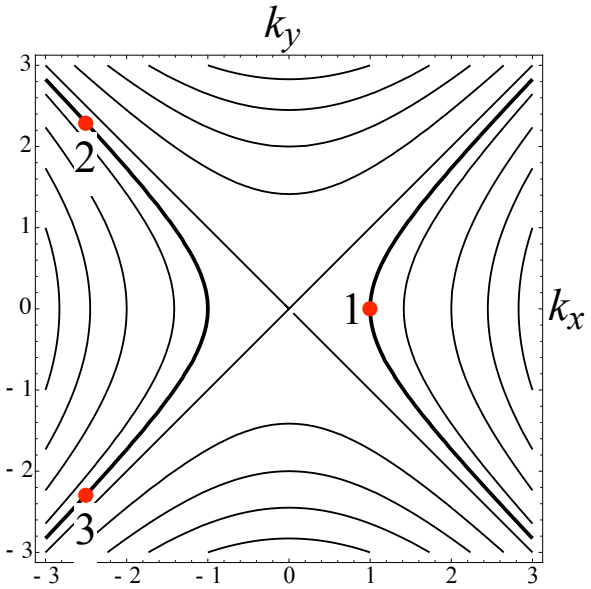

Figure 1. Constant-energy contours corresponding to (2.2). Contours for $|k_x| > |k_y|$ correspond to positive energies, and $|k_x| < |k_y|$ to negative energy; the bold curves represent $E = 1/2$. Dots indicate the plane waves in the superposition illustrated in section 5.

A convenient representation of these anisotropic plane waves, in terms of a parameter α, is

$$\psi_{\pm}(\boldsymbol{r};\alpha) = \exp\left(i\sqrt{2E}(\pm x\cosh\alpha + y\sinh\alpha)\right), (-\infty < \alpha < \infty). \qquad (2.3)$$

The parameter α is the counterpart of the plane-wave direction parameter θ in the more familiar solutions of $H_{\text{isotropic}}$, namely

$$\psi_{\text{isotropic}}(\boldsymbol{r};\theta) = \exp\left(i\sqrt{2E}(x\cos\theta + y\sin\theta)\right), (0 \le \theta < 2\pi)\,. \qquad (2.4)$$

3. Madelung streamlines: kinetic and canonical momentum

In Madelung's 'hydrodynamic' formulation of quantum theory [4], the wavefunction is expressed in polar form,

$$\psi(\boldsymbol{r}) = \rho(\boldsymbol{r})\exp\big(i\chi(\boldsymbol{r})\big), \qquad (3.1)$$

and the phase gradient

$$\boldsymbol{u}(\boldsymbol{r}) = \nabla\chi(\boldsymbol{r}) = \text{Im}\left(\frac{\nabla\psi(\boldsymbol{r})}{\psi(\boldsymbol{r})}\right) = \frac{\text{Im}\big(\psi^*(\boldsymbol{r})\nabla\psi(\boldsymbol{r})\big)}{|\psi(\boldsymbol{r})|^2}. \qquad (3.2)$$

is regarded as fundamental. One reason is that (after $\hbar$ scaling that we do not emphasise here – see the discussion after (1.2)) $\boldsymbol{u}(\boldsymbol{r})$ can be interpreted as a local, i.e. $\boldsymbol{r}-$ dependent, canonical momentum, in the following way. Using (1.1), and modifying the usual momentum expectation value by a δ function restricting position to r, and symmetrising to preserve Hermiticity, leads to the result

$$\boldsymbol{u}(\boldsymbol{r}) = \frac{1}{|\psi(\boldsymbol{r})|^2}\int_{-\infty}^{\infty} d\boldsymbol{r}'\psi^*(\boldsymbol{r}')\tfrac{1}{2}\big(\delta(\boldsymbol{r}'-\boldsymbol{r})\boldsymbol{p} + \boldsymbol{p}\delta(r'-r)\big)\psi(\boldsymbol{r}). \qquad (3.3)$$

A simple calculation shows that this is equivalent to (3.2). Several other formulations support this interpretation [9]. Streamlines are the integral curves of the vector field $\boldsymbol{u}(\boldsymbol{r})$: tangent to the vector at every point. In this

sense, the hydrodynamic formulation provides a convenient picture of the wave, complementary to the more familiar Schrödinger represntation.

For isotropic Hamiltonians, $\boldsymbol{u}(\boldsymbol{r})$ is also the kinetic momentum, interpretable (again after scaling with $\hbar$, and also mass) as a local particle velocity. But this is not the case for the anisotropic H considered here. This can be anticipated classically: from the first Hamilton equation, the velocity of a particle is proportional not to the canonical momentum but the kinetic momentum:

$$\boldsymbol{v}(t) = d_t\boldsymbol{r}(t) = \nabla_{\boldsymbol{p}}H = \big(p_x, -p_y\big). \tag{3.4}$$

(In waves, $\boldsymbol{v}(t)$is the group velocity of a wavepacket.) It is worth mentioning that even for isotropic Hamiltonians the canonical momentum $\boldsymbol{u}$ is gauge-dependent, in the following sense. Any free-particle Hamiltonan can be modified by adding a vector potential $\boldsymbol{A}(\boldsymbol{r})$, which provided it is curl-free, i.e. $\nabla \times \boldsymbol{A}(\boldsymbol{r}) = 0$, does not represent a magnetic field and so leads to the same physics. But $\boldsymbol{A}(\boldsymbol{r})$ changes the phase $\chi(\boldsymbol{r})$, and therefore the canonical momentum $\boldsymbol{u}(r)$. By contrast, the kinetic momentum $\boldsymbol{v}(\boldsymbol{r})$is unaffected by adding a curl-free vector potential.

This suggests that the quantum local kinetic momentum, proportional to the local velocity, is

$$\boldsymbol{v}(\boldsymbol{r}) = \Big(\partial_x\chi(r), -\partial_y\chi(r)\Big). \tag{3.5}$$

This interpretation is supported by the Madelung formulation, revisited in Appendix A, also by the interpretation of local velocity in the sense of (3.3), with $\boldsymbol{p}$ replaced by the commutator $[\boldsymbol{r}, H]$. Indeed, for anisotropic Hamiltonians, it is $\boldsymbol{v}$, not $\boldsymbol{u}$, that satisfies a continuity equation:

$$\nabla \cdot \big(\rho(r)^2\boldsymbol{v}(r)\big) = \rho(\boldsymbol{r})^2\nabla \cdot \boldsymbol{v}(\boldsymbol{r}) + (\nabla\rho(\boldsymbol{r})^2) \cdot \boldsymbol{v}(\boldsymbol{r}) = 0. \tag{3.6}$$

And if $\boldsymbol{v}(\boldsymbol{r})$ is regarded as a local quantum velocity, defined as

$$d_t \boldsymbol{r}(t) \equiv \boldsymbol{v}\big(\boldsymbol{r}(t)\big)\,, \tag{3.7}$$

its corresponding acceleration satisfies a modified Newton equation,

$$d_{tt}\boldsymbol{r}(t) = \boldsymbol{v}\big(\boldsymbol{r}(t)\big)\cdot\nabla\boldsymbol{v}\big(\boldsymbol{r}(t)\big) = -\begin{pmatrix}1 & 0\\ 0 & -1\end{pmatrix}\cdot\nabla V_Q\big(\boldsymbol{r}(t)\big), \tag{3.8}$$

involving the 'quantum potential'

$$V_Q(\boldsymbol{r}) = \frac{\partial_{yy}\rho(\boldsymbol{r}) - \partial_{xx}\rho(\boldsymbol{r})}{2\rho(\boldsymbol{r})}. \tag{3.9}$$

(In the Madelung quantum potential for the familiar isotropic Hamiltonians, the ∂_{yy} term is negative, so the potential involves $-\nabla^2$.)

For the time-independent solutions considered here, the streamlines of the vector field $\boldsymbol{v}(\boldsymbol{r})$ are the quantum trajectories of the particles with dynamics determined by (3.8). In (3.8) the gradient of the quantum potential expresses how quantum trajectories differ from their classical counterparts. As in the isotropic case, this quantum potential, depending on the wave intensity $\rho^2(\boldsymbol{r})$, means that even for propagation in free space the quantum trajectories can be curved, unlike the classical paths, which are straight.

There is a fundamental difference between the classical velocity (3.4) and the quantum velocity (3.5). Each classical trajectory can be considered in isolation, but quantum trajectories form families, determined by the velocity field $\boldsymbol{v}(\boldsymbol{r})$ associated with the wavefunction $\psi(\boldsymbol{r})$ and coupled to the intensity field $\rho^2(\boldsymbol{r})$.

4. Streamlines near phase singularities and phase saddles

For complex functions $\psi(\boldsymbol{r})$, zeros in the $\boldsymbol{r}$ plane are points, around wich the phase typically increases by $\pm 2\pi$. In the polar representation (3.1), $\rho = 0$, and the phase χ is undefined: zeros are phase singularities [10-17], currently extensively studied in the optics of structured light [18]. The

constant-phase contours - wavefronts - emerge from the singularity like spokes of a wheel (or like time zone boundaries at the poles of Earth, where all time zones meet).

Near such a zero, the coordinate dependence is linear:

$$\psi(\boldsymbol{r}) = ax + by + \cdots, \tag{4.1}$$

involving complex constants a, b. From (3.2) and (3.5), the canonical momentum and kinetic velocity are

$$\boldsymbol{u}(\boldsymbol{r}) = \frac{\mathrm{Im}(a^* b)}{|\psi(\boldsymbol{r})|^2}(-y, x), \qquad \boldsymbol{v}(\boldsymbol{r}) = -\frac{\mathrm{Im}(a^* b)}{|\psi(\boldsymbol{r})|^2}(y, x). \tag{4.2}$$

It follows that the $\boldsymbol{u}$ streamlines are circles ($\boldsymbol{u} \cdot \boldsymbol{r} = 0$); that is why phase singularities are wave vortices [19], the subject of much experimental and theoretical activity in optics [20, 21]. By contrast, the $\boldsymbol{v}$ streamlines are rectangular hyperbolas, with asymptotes $x^2 = y^2$ (where $\boldsymbol{v}$ and $\boldsymbol{r}$ are parallel, i.e. $\boldsymbol{v} \times \boldsymbol{r} = 0$).

The pattern of phase contours is also singular at places where ρ is not zero, namely phase saddles. Near such points, χ varies quadratically:

$$\chi(\boldsymbol{r}) = \chi_0 + \tfrac{1}{2}ax^2 + bxy + \tfrac{1}{2}cx^2, \tag{4.3}$$

in which the constants a, b, c are real. From the continuity equation (3.6), it follows that $\nabla \cdot \boldsymbol{v}(\boldsymbol{r}) = 0$ where $\boldsymbol{v} = 0$, implying $c = a$**.** Therefore the $\boldsymbol{u}$ and $\boldsymbol{v}$ fields near a saddle take the form

$$\boldsymbol{u}(\boldsymbol{r}) = (ax + by, bx + ay), \qquad \boldsymbol{v}(\boldsymbol{r}) = (ax + by, -bx - ay). \tag{4.4}$$

At a saddle, the two principal curvatures (eigenvalues of the quadratic form in (19) [22]) have opposite signs, so the Gaussian curvature is negative:

$$\det\begin{pmatrix} \partial_{xx}\chi & \partial_{xy}\chi \\ \partial_{yx}\chi & \partial_{yy}\chi \end{pmatrix} = a^2 - b^2 < 0\,. \tag{4.5}$$

It follows that the $\boldsymbol{u}$ streamlines are hyperbolas, generally not rectangular,, with asymptotes $x^2 = y^2$, and the $\boldsymbol{v}$ streamlines are ellipses, generally not circular, with principal axes $x^2 = y^2$.

These geometrical features can be understood in terms of the indices of the singularities of the line patterns associated with the fields: contours for χ and streamlines for $\boldsymbol{u}$ and $\boldsymbol{v}$. The index of a singularity of a line pattern is the signed number of times its lines rotate round a circuit of it [22]. Phase singularities have index +1 and phase saddles have index -1. At a phase vortex, the $\boldsymbol{u}$ pattern has index +1 and the $\boldsymbol{v}$ pattern has index -1; at a phase saddle, it is the opposite: the $\boldsymbol{u}$ pattern has index -1 and the $\boldsymbol{v}$ pattern has index +1

These geometrical features are illustrated in Figure 2 for a simple solution of (1.3), namely

$$\psi(r) = \left(y^2 - \tfrac{1}{4} - ix\right)\exp(ix), \tag{4.6}$$

which has phase vortices at $(0, \pm 1/2)$ and phase saddles at $\left(0, \pm\sqrt{5}/2\right)$.

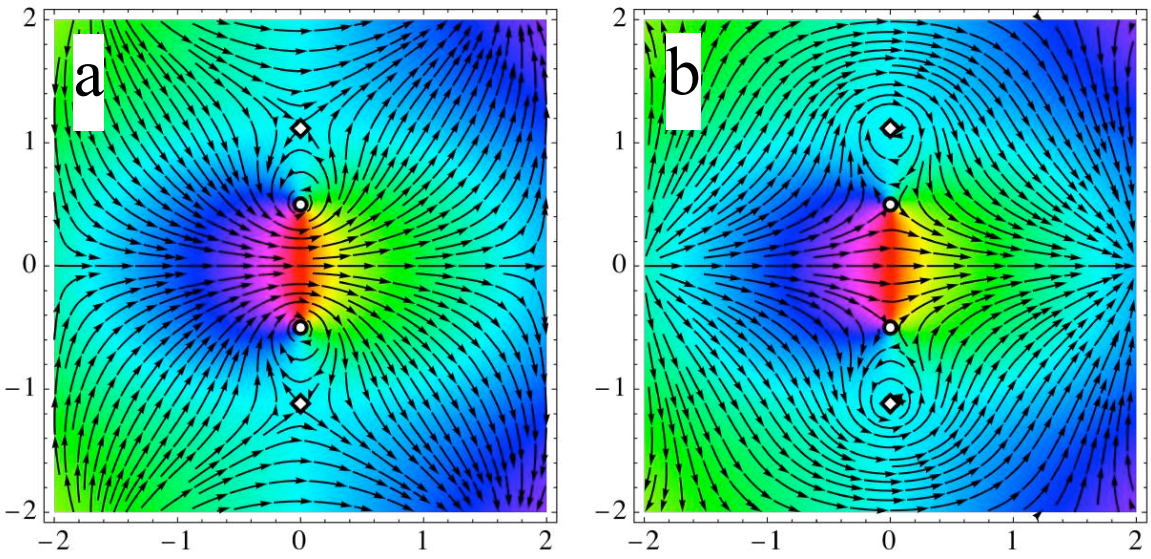

Figure 2. In both (a) and (b), the phase of (4,6) is colour-coded by HUE; all colours meet at phase singularities, where $\rho = 0$, denoted by circles; the phase saddles are denoted by diamonds. Superimposed are the streamlines

of (a), canonical momentum $\boldsymbol{u}(\boldsymbol{r})$, with vortices at the phase singularities and saddles at the phase saddles; (b) kinetic momentum $\boldsymbol{v}(\boldsymbol{r})$, with saddles at the phase singularities and vortices at the phase saddles.

5. A three-wave superposition

A superposition of three waves, namely

$$\psi(\boldsymbol{r}) = c_1 \exp(i\boldsymbol{k}_1 \cdot \boldsymbol{r}) + c_2 \exp(i\boldsymbol{k}_2 \cdot \boldsymbol{r}) + c_3 \exp(i\boldsymbol{k}_3 \cdot \boldsymbol{r}), \tag{5.1}$$

suffices to illustrate the rich patterns of streamlines that can occur. Figure 3 shows $\boldsymbol{u}(\boldsymbol{r})$ and $\boldsymbol{v}(\boldsymbol{r})$ for a wave with $E = 1/2$ and the following choice of wavevectors, α parameters in (6), and coefficients:

$$\begin{gathered} \boldsymbol{k}_1 = (1,0), \boldsymbol{k}_2 = (-2.5, 2.29129), \boldsymbol{k}_3 = (-2.5, -2.29129); \\ \alpha_1 = 0, \alpha_2 = \alpha_3 = -1.5668; |\boldsymbol{k}_1| = 1, |\boldsymbol{k}_2| = |\boldsymbol{k}_3| = 3.39116; \\ c_1 = 1, c_2 = \tfrac{1}{2}, c_3 = 1. \end{gathered} \tag{5.2}$$

In addition to the contrasting behaviour near phase singularites and phase saddles, both families of streamlines display the undulations indicative of interference in the Madelung formulation [4].

As well as phase singularities and phase saddles, the phase of solutions of kinetically anisotropic Hamiltonians can also possess phase extrema (maxima and minima); as discussed in Appendix B, these are relatively rare.

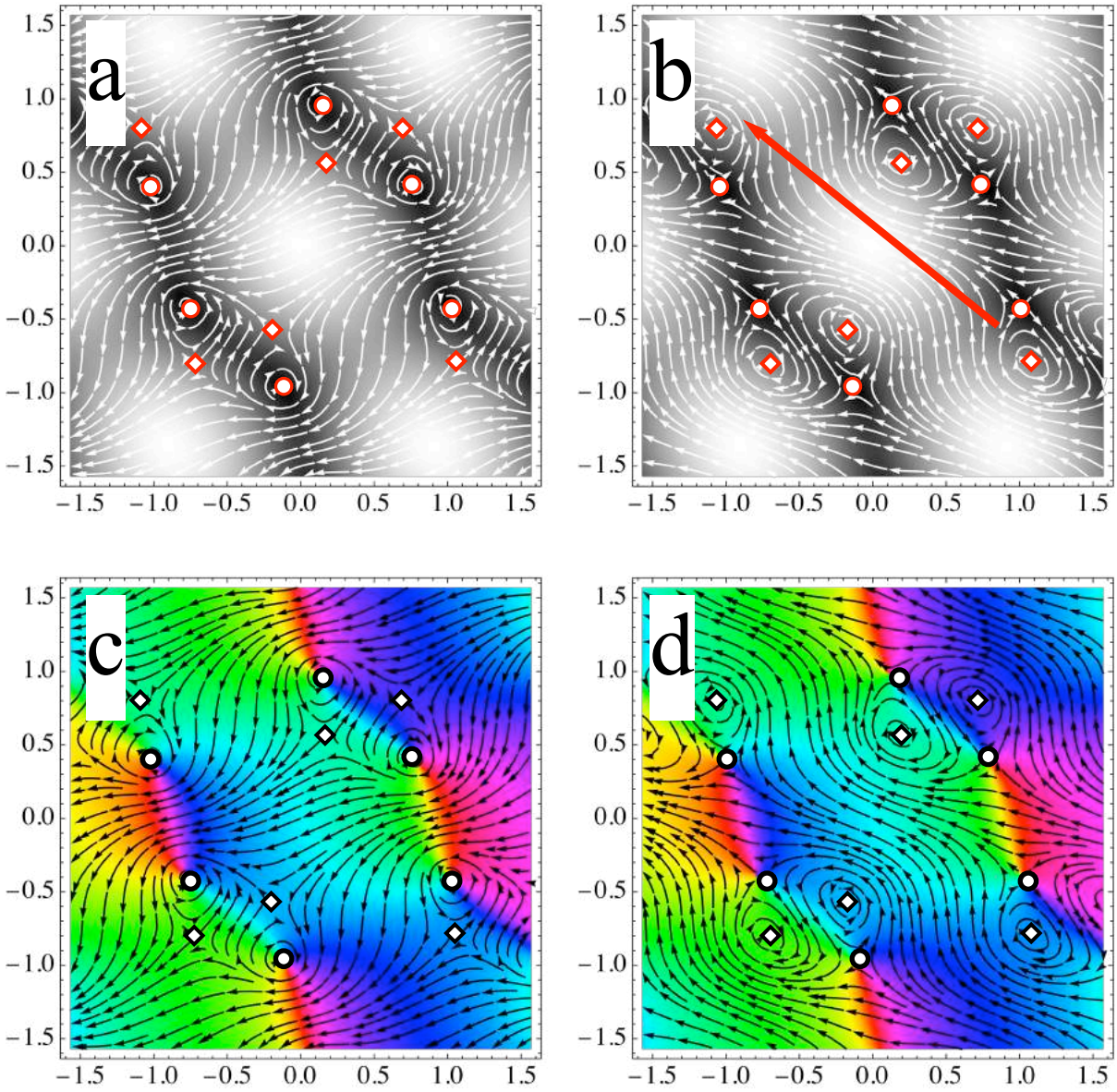

Figure 3. Streamlines for (a, c) $\boldsymbol{u}(\boldsymbol{r})$, and (b), d) $\boldsymbol{v}(\boldsymbol{r})$, for the three-wave superposition (5.1-5.2). In (a, b) the streamlines (white) are superimposed on the intensity $\rho^2(\boldsymbol{r})$ (grayscale, with high intensities white and zeros indicated by red circles and phase saddles by red diamonds); the red arrow in (b) represents the mean kinetic momentum; in (c, d) the streamlines (black) are superimposed on the phase (with zeros indicated by black circles and phase saddles by black diamonds), as in figure 2.

6. Singular eigenfunctions

For the isotropic Hamiltonian (1.2), the continuous superposition of plane waves (2.4) travelling in all directions θ leads to a circularly symmetric Bessel wave; for $E = 1/2$,

$$\psi_{\text{isotropic}}(\boldsymbol{r}) = \frac{1}{2\pi}\int_{-\pi}^{\pi} d\theta \exp\left(i\sqrt{2E}(x\cos\theta + y\sin\theta)\right) = J_0\left(\sqrt{2E(x^2+y^2)}\right) \tag{6.1}$$

This wave, which has no singularities, can also be regarded as the superposition of outgoing and incoming circular waves, is illustrated in Figure 4a. The analogous exact solution for the anisotropic Hamiltonian (1.3) would appear to be obtained by replacing y by $-y$:

$$\psi(\boldsymbol{r}) = J_0\left(\sqrt{2E(x^2-y^2)}\right). \tag{6.2}$$

But it is not acceptable, because for $y^2 > x^2$ the argument of the Bessel function is imaginary, and

$$\psi(\boldsymbol{r}) = I_0\left(\sqrt{y^2-x^2}\right), \tag{6.3}$$

where I_0 is the modified Bessel function, grows exponentially as $|y|$ increases. The reason is that in the superposition (6.1) the replacement $y \to iy$ involves exponentials that are real rather than complex, corresponding to evanescent/growing waves rather than the phase factors representing propagating waves.

However, it is possible to create a counterpart of (6.2) that is satisfactory in the sense that it does not diverge in any sector of the $\boldsymbol{r}$ plane. An instructive way to do this is via the propagator for the Hamiltonian (1.3), with the source at $\boldsymbol{r} = \boldsymbol{0}$. Using the momentum representation,

$$G(\boldsymbol{r},t) = \langle \boldsymbol{r}|\exp(-iHt)\,|\boldsymbol{0}\rangle = \frac{1}{(2\pi)^2}\iint d\boldsymbol{k}\exp\left(i\boldsymbol{k}\cdot\boldsymbol{r} - \tfrac{1}{2}i\left(k_x^2 - k_y^2\right)t\right). \tag{6.4}$$

The integration is over the $\boldsymbol{k}$ plane, and the two Gaussian integrals give

$$G(\boldsymbol{r},t)=\frac{\exp\left(i\dfrac{x^2-y^2}{2t}\right)}{2\pi t}\,. \tag{6.5}$$

The desired counterpart of (6.2) is

$$\psi(\boldsymbol{r})=2\,\mathrm{Im}\int_0^\infty dt\,\exp(iEt)G(\boldsymbol{r},t)=\frac{1}{\pi}\int_0^\infty\frac{dt}{t}\sin\left(Et+\frac{x^2-y^2}{2t}\right). \tag{6.6}$$

(The real part gives a singular solution representing a source at $\boldsymbol{r}=\boldsymbol{0}$.) As shown in Appendix C, the integral reduces a standard representation of the Bessel function (6.2), with the difference that it vanishes in the regions $y^2 \gtrless x^2$ for $E \gtrless 0$

$$\psi(\boldsymbol{r})=J_0\left(\sqrt{2E(x^2-y^2)}\right)\Theta\big(E(x^2-y^2)\big), \tag{6.7}$$

in which Θ denotes the unit step. The wave is ilustrated in Figure 4b.

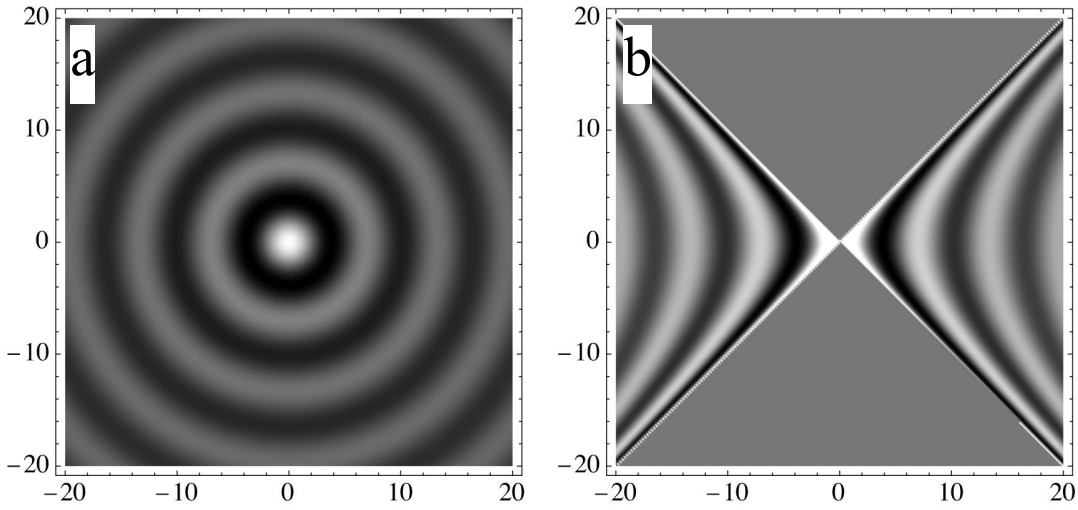

Figure 4. (a) Isotropic Bessel wave (6.1); (b) anisotropic Bessel wave (6.7).

The discontinuity of (6.7) across the lines $|y|=|x|$ is unfamiliar, and threatens its validity as a legitimate solution of (1.3). Demonstrating that in fact the discontinuous function is a solution is an instructive exercise in the manipulation of step and delta functions. Define the discrepancy

$$\Delta\psi(x,y) \equiv \left(-\partial_{xx} + \partial_{yy} - 2E\right)\psi(\boldsymbol{r})\,. \tag{6.8}$$

This should vanish everywhere for all E. An explicit calculation, using (1.3), with $2E = 1$ for convenience, gives, after using $\Theta'(u) = \delta(u)$,

$$\begin{aligned}\Delta\psi(x,y) = \frac{4J_1\left(\sqrt{x^2-y^2}\right)}{\sqrt{x^2-y^2}}(x^2-y^2)\delta(x^2-y^2)\\ -4J_0\left(\sqrt{x^2-y^2}\right)\left(\delta(x^2-y^2) + (x^2-y^2)\delta'(x^2-y^2)\right).\end{aligned} \tag{6.9}$$

The first term on the r.h.s. vanishes because $u\delta(u) = 0$. The second term vanishes too, because use of $\delta'(u^2) = \delta'(u)/(2u)$ and $f(u)\delta'(u) = -f'(u)\delta(u)$ leads to

$$(x^2-y^2)\delta'(x^2-y^2) = -\delta(x^2-y^2). \tag{6.10}$$

Therefore this formal argument gives

$$\Delta\psi(x,y) = 0\,. \tag{6.11}$$

A more detailed analysis, based on smoothing the step in (6.7) , evaluating the discrepancy $\Delta\psi(x,y)$, and then resharpening, leads to the same result.

Worth noting is that the propagator integral (6.6) can be expressed as a superposition of the plane waves (2.3). After transforming the integration variable by

$$t = \frac{|x| + y}{\sqrt{2E}}\exp u, \tag{6.12}$$

(6.6) becomes, after a short calculation,

$$\psi(\boldsymbol{r}) = \frac{1}{\pi}\int_{-\infty}^{\infty} du \sin\left(\sqrt{2E}(|x|\cosh u + y\sinh u)\right). \tag{6.13}$$

This is indeed a superposition of plane waves. Moreover, numerical approximation as a discrete superposition, replacing the integral as a sum, with $u = n\delta, -N \le n \le N, \delta \ll 1, N \gg 1, N\delta \gg 1$, reproduces figure 4b to

visual accuracy, including its discontinuities. I do not give details, but suggest $\delta = 0.02, N = 200$ for students seeking to explore the superposition.

To demystify the unexpected result that an eigenstate of the Schrödinger equation (1.3) for a free particle in 2D can be discontinuous, note that the replacements $x \to t, y \to x,\ 2E \to m^2$ gives

$$(\partial_{tt} - \partial_{xx} + m^2)\psi = 0. \tag{6.12}$$

This is the Klein-Gordon equation for the evolution of the state of a relativistic particle moving in one space dimension. The step in (6.7) restricts the particle to lie within the light cone $|x| \leq |t|$, i.e. the evolution is causal (for further analysis of this kind of causal evolution, and a related discussion of discontinuities, see [23, 24]).

For simplicity of exposition, we have deliberately chosen to illustrate anisotropisation using the simplest Bessel wave (6.1). But it is easy to extend the process to the more general wave

$$\psi_{m,\text{isotropic}}(\boldsymbol{r}) = J_{|m|}\left(\sqrt{2E(x^2+y^2)}\right)\exp(im\theta)\,. \tag{6.13}$$

Again with the replacement $y \to iy$, now with the cutoff for $y^2 > x^2$, and using

$$\exp(i\theta) = \frac{x+iy}{\sqrt{x^2+y^2}} \to \frac{x-y}{\sqrt{x^2-y^2}}\,, \tag{6.14}$$

gives the generalisation of (6.7):

$$\psi_m(\boldsymbol{r}) = \frac{J_{|m|}\left(\sqrt{2E(x^2-y^2)}\right)}{(x^2-y^2)^{\frac{m}{2}}}(x-y)^m\Theta\big(E(x^2-y^2)\big). \tag{6.15}$$

The argument around (6.8)-(6.11), demonstrating that the cutoff does not spoil the solution, generalises, and then it is easy to show that the

waves (6.15) are exact solutions of (1.3). The singlevaluedness of (6.13), restricting m to be integer, no longer applies, so the index m can take any real value. The factor $(x - y)$ means that for $m > 0, E > 0, x > 0$ these waves are small at the upper boundary cutoff $y = +x$ and large on the lower boundary $y = -x$, with the opposite for $x < 0$. The replacement $m \to -m$ replaces $(x - y)$ by $(x + y)$, so for $m < 0$ the large/small behaviour at the cutoffs is reversed.

7. Concluding remarks

Emerging from this study of the simplest kinetically anisotropic Hamiltonian are several examples of phenomena familiar in isotropic Hamiltonians appearing in unfamilar guises. In previous work, tacitly restricted to isotropic Hamiltonians, streamlines circulate around phase singularities, in the long-studied wave vortices [10, 11], and are hyperbolic close to phase saddles [25]. For anisotropic Hamiltonians, where canonical and kinetic momenta are different, the association between phase geometry and streamlines is the opposite: hyperbolic streamlines at the phase singularities and circulating streamlines around the phase saddles. And instead of the smooth eigenfunctions of isotropic Hamiltonians, in the anisotropic Hamiltonian studied here there are eigenstates that are discontinuous functions of position.

For simplicity of exposition, only the simplest anisotropic Hamiltonian has considered. But the unfamilar phenomena survive generalisation: for example, to anisotropic hamiltonians whose kinetic contributions have opposite signs but not necessarily the same magnitudes; or which involve external forces, represented by a potential; or in more than two dimensions.

Finally, the analysis provides examples that could be useful in graduate-level teaching of a number of important concepts and techniques. These include

• The difference between canonical and kinetic momenta;

• Madelung streamlines;

• Phase;

• Geometrical features, such as index, associated with singularities of line patterns;

• Manipulations of step functions and delta functions.

Acknowledgments. I thank Professor John Hannay and Professor Pragya Shukla for many helpful discussions.

Appendix A. Madelung formalism for anisotropic Hamiltonian

This is a reprise of the argument in Appendix A of [26], which deals with a slightly more general case. Substitution of the polar representation (3.1) into the Schrödinger equation (1.3) leads, after separating real and imaginary parts, to two equations connecting ρ and χ.

The imaginary part gives the continuity equation (3.6), involving the kinetic $\boldsymbol{v}$ rather than the canonical $\boldsymbol{u}$. The real part leads, after some calculation, to

$$\frac{1}{2}\boldsymbol{u}(\boldsymbol{r})\cdot\boldsymbol{v}(\boldsymbol{r})+V_Q(\boldsymbol{r})=E, \tag{A. 1}$$

involving the quantum potential (3.9). The Newton equation (3.8) is obtained by taking the gradient. A crucial step involves the relation

$$(v\cdot\nabla)v=\begin{pmatrix}1 & 0\\ 0 & -1\end{pmatrix}\cdot\nabla\left(\frac{1}{2}\boldsymbol{u}\cdot\boldsymbol{v}\right)=\begin{pmatrix}\partial_x\\ -\partial_y\end{pmatrix}\left(\frac{1}{2}\boldsymbol{u}\cdot\boldsymbol{v}\right), \tag{A. 2}$$

whose proof follows from the fact that $\boldsymbol{u}$ is irrotational because it a gradient.

Appendix B. Phase extrema

Consider a general complex function in the plane: $\psi(\boldsymbol{r}), \boldsymbol{r} = (x, y)$. There are phase singularities where $|\psi| = 0$, and also phase saddles and phase extrema (maxima or minima) where $\nabla \arg \psi = \nabla\chi = \boldsymbol{u} = \boldsymbol{v} = 0$ (the zeros of $\boldsymbol{u}$ coincide with those of $\boldsymbol{v}$, cf. (3.2) and (3.5)). Saddles and extrema are stationary points of the phase, which can be written in the form (4.3). Saddles correspond to negative Gaussian curvature of χ, i.e. $ac - b^2 < 0$, and extrema to positive Gaussian curvature, i.e. $ac - b^2 > 0$.

But the functions considered here are not general: they are constrained by being solutions of wave equations. For the familiar kinetically isotropic Hamiltonians, e.g. (1.2), Madelung continuity implies $\nabla \cdot \boldsymbol{u} = 0$, and therefore $c = -a$. The Gaussian curvature is $-a^2 - b^2$, which can never be positive, so there are no phase extrema [25].

For the kinetically anisotropic Hamiltonians considered here, continuity implies $\nabla \cdot \boldsymbol{v} = 0$, implying $c = +a$ (cf. the text following (4.3)) and the Gaussian curvature (4.5), which is negative for phase saddles, as studied in detail. But there is no restriction preventing $a^2 > b^2$, leaving open the possibility of phase extrema.

These do occur but seem rare. I explored many few-wave superpositions, searching for places where $\boldsymbol{u} = 0$ in regions with positive Gaussian curvature. Usually these conditions were not satisfied, but I found a five-wave superposition with two very shallow phase extrema: a phase maximum and a nearby phase minimum.

An approach to a theory of phase extrema would be to consider random solutions of (1.3), for example superpositions of many plane waves

(2.3) with random phases and amplitudes, and calculate the probability that a stationary point of phase would be an extremum rather than a saddle. There have been many calculations of geometrical statistics of waves [27-29]. Somewhat similar to the present example is the statistics of different types of umbilic point; these are places where the two principal curvatures are equal, and there is a threefold classification [30], playing a role in optics [11]; it was found that one of the types – 'monstars' – is rather rare (probablility 0.053).

The patterns considered here do not exhaust the possibilities. For approximations to solutions of the time-independent wave equations, streamlines near phase singularities can form spirals rather than closed loops [31], and Madelung streamlines for time-dependent waves avoid each phase singularity in spacetime, except for one that meets it in a cusp [31, 32].

Appendix C. Derivation of (6.7) from (6.6)

Replace the integration variable t by s, where

$$t = \sqrt{\left|\frac{x^2 - y^2}{2E}\right|}\, s. \qquad \text{(C. 1)}$$

This brings (6.6) to the symmetrical form

$$\psi(\boldsymbol{r}) = \frac{1}{\pi}\int_0^\infty \frac{ds}{s} \sin\left(\frac{1}{2}|X|\left(s + \frac{1}{s}\,\mathrm{sign}\big(E(x^2 - y^2)\big)\right)\right), \qquad \text{(C. 2)}$$

where

$$X = \sqrt{2E(x^2 - y^2)}\,. \qquad \text{(C. 3)}$$

With the negative sign, the argument of the sine is $s - 1/s$, and the transformation $s \to 1/s$ gives

$$E(x^2 - y^2) < 0 \Longrightarrow \psi(\boldsymbol{r}) = -\psi(\boldsymbol{r}) = 0. \qquad \text{(C. 4)}$$

With the positive sign, the same transformation shows that the contributions from $0 < s \leq 1$ and $1 \leq s < \infty$ are the same, so

$$\psi(\boldsymbol{r}) = \frac{2}{\pi}\int_1^\infty \frac{ds}{s}\sin\left(\frac{1}{2}X\left(s + \frac{1}{s}\right)\right). \qquad \text{(C. 5)}$$

The final transformation $s + 1/s = 2w$ leads to

$$\psi(\boldsymbol{r}) = \frac{2}{\pi}\int_1^\infty \frac{dw}{\sqrt{w^2 - 1}}\sin(Xw), \qquad \text{(C. 6)}$$

which is a standard integral representation of $J_0(X)$ (e.g. formula 10.9.11 of [33]).

References

[1] Berry, M. V., & Shukla, P. 2015 Hamiltonian curl forces *Proc. R. Soc. A* **471** 20150002 (20150013pp).

[2] Blakemore, J. S. 1985.*Solid State Physics (2nd. Edition)* Cambridge: University Press

[3] Poddubny, A., Iorsh, I., Belov, P., Kivshar, Y. 2013 Hyperbolic metamaterials *Nature Photonics* **7** 958-967.

[4] Madelung, E. 1927 Quantentheorie in Hydrodynamische Form *Z. für Phys.* **40** 322-326. Translation is available at https://neo-classical-physics.info/uploads/3/4/3/6/34363841/madelung_-_hydrodynamical_interp..pdf

[5] Takabayasi, T. 1954 The formulation of quantum mechanics in terms of ensemble in phase space *Proc. Theor. Phys. Jap.* **11** 341-373.

[6] Heifetz, E., & Cohen, E. 2015 Toward a Thermo-hydrodynamic Like Description of Schrödinger Equation via the Madelung Formulation and Fisher Information *Found. Phys.* **45** 1514-1525.

[7] Heifetz, E., & Cohen, E. 2020 Madelung transformation of the quantum bouncer problem *EPL* **130** 10002.

[8] Foskett, M. S., & Tronci, C. 2022 Holonomy and vortex structures in quantum hydrodynamics, in 'Hamiltonian Systems: Dynamics, Analysis, Applications', eds: A.Fathi,P.J Morrison, T-M Seara, S. Tabachnikov *Math. Sci. Res. Inst. Pub.* **72** 101-142. Retrieved from arXiv:2003.08664v3 [math-phys] 6 Mar

[9] Berry, M. V. 2013 Five momenta *Eur. J. Phys.* **44** 1337-1348.

[10] Nye, J. F., & Berry, M. V. 1974 Dislocations in wave trains *Proc. Roy. Soc. Lond.* **A336** 165-190.

[11] Nye, J. F. 1999.*Natural focusing and fine structure of light: Caustics and wave dislocations* Bristol: Institute of Physics Publishing

[12] Hirschfelder, J. O., Christoph, A. C., & Palke, W. E. 1974 Quantum mechanical streamlines. 1. Square potential barrier *J. Chem. Phys.* **61** 5435-5455.

[13] Hirschfelder, J. O., Goebel, C. G., & Bruch, L. W. 1974 Quantum mechanical streamlines. 1. Square potential barrier *J. Chem. Phys.* **61** 5421-5425.

[14] Hirschfelder, J. O., & Tang, K. T. 1976 Quantum mechanical streamlines. III Idealized reactive atom-diatomic molecule collision *J. Chem. Phys.* **64** 760-785.

[15] Hirschfelder, J. O., & Tang, K. T. 1976 Quantum mechanical streamlines. IV. Collision of two spheres with square potential wells or barriers *J. Chem. Phys.* **65** 470-486.

[16] Riess, J. 1970 Nodal structure of Schroedinger wave functions and its physical significance *Ann. Phys. (NY)* **57** 301-321.

[17] Riess, J. 1970 Nodal structure, nodal flux fields, and flux quantization in stationary quantum states *Phys. Rev .D.* **2** 647-653.

[18] Rubinsztein-Dunlop, H., & others. 2017 Roadmap on Structured light *J.Optics* **18** 013001 (013051pp).

[19] Berry, M. V. 1998 Much ado about nothing: optical dislocation lines (phase singularities, zeros, vortices…) in *Singular Optics* (Ed: Soskin, M.S.), Frunzenskoe, Crimea *SPIE* **3487** 1-5.

[20] Dennis, M. R., O'Holleran, K., & Padgett, M. J. 2009 Singular Optics: Optical Vortices and Polarization Singularities *Progress in Optics* **53** 293-363.

[21] Soskin, M. S., & Vasnetsov, M. V. 2001 Singular Optics *Progress in Optics* **42** 219-276.

[22] Needham, T. 2021.*Visual Differential Geometry and Forms; A mathematical drama in five acts* Princeton: University Press

[23] Berry, M. V. 2012 Causal wave propagation for relativistic massive particles *Eur. J. Phys.* **33** 279-294.

[24] Bliokh, K. Y. 2018 Lorentz-boost eigenmodes *Phys. Rev. A* **98** 012143.

[25] Nye, J. F., Hajnal, J. V., & Hannay, J. H. 1988 Phase saddles and dislocations in two-dimensional waves such as the tides *Proc. Roy. Soc. Lond.* **A417** 7-20.

[26] Berry, M. V., & Shukla, P. 2023 Quantum curl forces *J, Phys. A* **56** 485206 (485224pp).

[27] Longuet-Higgins, M. S. 1956 Statistical properties of a moving waveform *Proc. Camb. Phil. Soc.* **52** 234-245.

[28] Longuet-Higgins, M. S. 1958 The statistical distribution of the curvature of a random Gaussian surface *Proc .Camb. Phil. Soc.* **54** 439-453.

[29] Berry, M. V., & Dennis, M. R. 2000 Phase singularities in isotropic random waves *Proc. R. Soc. A* **456** 2059-2079, corrigenda in A2456 p3048.

[30] Berry, M. V., & Hannay, J. H. 1977 Umbilic points on Gaussian random surfaces *J. Phys. A* **10** 1809-1821.

[31] Berry, M. V. 2005 Phase vortex spirals *J. Phys. A* **38** L745-L751.

[32] Berry, M. V. 2024 Time-independent, paraxial and time-dependent Madelung trajectories near zeros *J. Phys. A* **57** 025201 (025211pp).

[33] DLMF 2010.*NIST Handbook of Mathematical Functions* Cambridge: University Press